



Observation of superfluorescence from a quantum ensemble of coherent excitons in a ZnTe crystal: Evidence for spontaneous Bose-Einstein condensation of excitons

D. C. Dai* and A. P. Monkman

Department of Physics, Durham University, South Road, Durham DH1 3LE, United Kingdom

(Received 26 July 2011; published 19 September 2011)

Superfluorescence (SF) is the emission from a dense coherent system in population inversion formed from an initially incoherent ensemble. This is characterized by an induction time (τ_D) for the spontaneous development of the macroscopic quantum coherence. Here we report detailed observation of SF on an ultrafast timescale from a quantum ensemble of coherent excitons in highly excited intrinsic-bulk ZnTe single crystal at 5 K, showing a characteristic τ_D from 40 ps to 10 ps, quantum noise and fluctuations, and quantum beating and ringing. From this clear observation of SF from a spontaneous coherence of excitons bound to impurities and defect states, we infer that this is indicative of the formation of a spontaneous Bose-Einstein condensation (BEC) of excitons on an ultrafast timescale. The population density and dephasing time (T_2 or T_2^*) of exciton are two controlling factors in the generation of SF from the BEC.

DOI: [10.1103/PhysRevB.84.115206](https://doi.org/10.1103/PhysRevB.84.115206)

PACS number(s): 78.47.jd, 42.50.Nn, 05.30.Jp, 42.50.Md

I. INTRODUCTION

Superfluorescence (SF) and super-radiance (SR) are both forms of cooperative emission arising from a dense coherent ensemble (N_c) in a population inversion (N) first predicted by Dicke in 1954¹ and subsequently termed by Bonifacio and Lugiato in 1975.² If a dense population inversion has an initial macroscopic polarization, as created coherently by a laser ($N = N_c$), for example, the resultant emission is SR. However, in some cases, an initially incoherent dense N can form spontaneous coherence over a subset of excited states N_c with a unique characteristic induction time τ_D resulting in SF.^{2,3} In contrast amplified spontaneous emission (ASE) is the collective emission from a purely incoherent dense N .⁴ Although SF, SR, and ASE are all observed as mirrorless lasing in the absence of a laser cavity, SF differs essentially from SR and ASE by the existence of τ_D for the development of macroscopic spontaneous quantum coherence.²⁻⁴ In order to resolve the SF process in experiment both the duration of the excitation pulse (τ_p) and the time resolution of the emission detection system (Δt) must be shorter than τ_D , i.e., $(\tau_p, \Delta t) < \tau_D$.⁵⁻¹¹ Also SF has the observable features of emission-line narrowing, greatly increased intensity, quantum noise and quantum fluctuations, quantum beating and ringing, etc. It also follows the relationships $I_{SF} \propto N_c^2$, $\tau_R = (8\pi/3N_c\lambda^2l)\tau_{SP}$, and $\tau_D = \tau_R[\ln(2\pi S l N_c)^{1/2}]^2/4$, where τ_{SP} is the lifetime of spontaneous emission, I_{SF} and τ_R are respectively the intensity and characteristic radiation time of SF emission at the wavelength λ , and S and l are the area and thickness of the gain medium, respectively.¹⁻¹⁰

SF emission from the whole coherent ensemble of N_c is triggered by a random individual spontaneous emission event within N_c due to quantum fluctuations,⁶⁻⁹ therefore the properties of SF (such as τ_D , pulse shape, and intensity) fluctuate from shot to shot, i.e., exhibiting quantum noise.^{3,5,6} SF is particularly interesting because it is intrinsically a quantum mechanical phenomenon and provides a significant tool to study the quantum coherence and the macroscopic quantum fluctuations in the time domain.³ Importantly, τ_D is always limited by the dephasing time, T_2 or T_2^* , which always acts to destroy the coherence⁶⁻¹⁰ and is defined by

the inverse of the transition cross-sections in homogeneous or inhomogeneous systems, respectively. Thus SF has a key criterion: $(\tau_R \tau_D)^{1/2} < T_2^*$.⁷⁻⁹

Given that SF is the signature of a spontaneous development of a coherent exciton ensemble, we think this can be viewed as a Bose-Einstein condensation (BEC) of the excitons through spontaneous symmetry breaking. The convincing observation of an excitonic BEC in a semiconductor is a long held but unresolved issue from its prediction in 1962.¹²⁻¹⁷ Practically all of the previous claims have been disputed due to the lack of unique evidence.^{16,17} One of the key issues is the experimental proof of the formation of the spontaneous macroscopic Bose coherence,¹⁷ which has been well attested in superfluidity, superconductivity, and atomic BEC.^{13,18} A drawback in experiments is the short lifetime of the excitons, which is on ultrafast timescale (usually on the order of magnitude of 100 ps), within which the condensation is expected to occur.¹²⁻¹⁷ SF from a quantum coherent ensemble of excitons should be an excellent way of demonstrating the BEC of excitons, however, this has not been previously suggested in theoretical work, nor has it been successfully observed in a semiconductor so far. Here we directly address this issue.

From the first observation of SF from highly excited HF gas,⁶ many other gaseous atomic or molecular systems with predominantly homogeneous line broadening have been unambiguously found to emit SF.⁵⁻⁹ There are only a few reports of SF in the crystalline solid phase with inhomogeneous broadening, of which the most documented is KCl:O₂⁻,^{10,11} and Jho *et al.* reported observations of SF from GaAs quantum wells using steady-state spectroscopy combined with high magnetic fields.^{19,20} In other reported cases the experimental evidence (lack of a unique τ_D , for example) has not substantiated SF. These include ruby:Cr³⁺,²¹ GaAs laser diodes,²² ZnO materials,²³⁻²⁶ CuCl quantum dots,²⁷ WO_{3-x} nanowires,²⁸ diphenyl:pyrene,²⁹ R-phycoerythrin,³⁰ and thiophene/phenylene co-oligomer.³¹

ZnTe crystals, as the model II-VI direct-gap intrinsic semiconductor, have been used to attempt to observe BEC of excitons,³² and efforts have been made to resolve the lasing behavior from highly excited ZnTe epitaxial layers

with a $\tau_p = 70$ ps.³³ Here we report exciton dynamics with femtosecond resolution in ZnTe crystals at 5 K studied by the femtosecond time-resolved fluorescence technique, showing clear observation of SF emission. A characteristic τ_D , together with the associated features of quadratic power dependence, quantum noise and quantum fluctuations, quantum beating and ringing, are all observed.

II. EXPERIMENTAL METHODS

ZnTe has a band gap (E_g) of 2.26 eV at room temperature and 2.38 eV at 4.2 K, respectively. The yellow-orange colored ZnTe (110) single crystals used in our experiments, having a pair of slightly wedged polished surfaces (size 5 mm \times 5 mm), were purchased from Ingcrys Laser Systems Ltd (www.ingcrys.com). The information from the provider states that these ZnTe crystals are made in Russia by seeded vapor-phase free growth, performed in sealed-off or quasiclosed quartz ampoules by use of physical transport in He or Ar gas flow at the temperature = 1080–1150 °C. In experiments the crystal is mounted in a closed-cycle Helium cryostat, and the lowest temperature is at 5.0 K; other temperatures up to room temperature can be kept at the range of ± 0.25 K. The cryostat is mounted on a manual Y-Z stage, which allows continuous movement of laser spot on the crystal surface without violating the optical path and shifting the time delay.

The femtosecond time-resolved fluorescence up-conversion technique can provide a time-resolution (Δt) of up to a few fs, which is mainly limited by the duration (τ_p) of laser pulse employed.^{34–37} The laser source used in our experiments is a commercial $\tau_p = 180$ fs amplifier (Coherent RegA 9000), which delivers a 5.0- μ J pulse at 100 KHz and 780 nm (1.59 eV). The pump laser at $\lambda_{ex} = 390$ nm (3.18 eV), the second harmonic (SHG) of 780 nm, is focused by a singlet lens onto the sample ZnTe crystal at an incident angle of $\sim 3^\circ$; the diameter of the laser spot is $D = 100$ μ m. The forward emission is collected by another singlet lens and converged onto a Beta Barium Borate (BBO) crystal, where the emission

is up-converted in a cross-linear geometry by a gating beam at 780 nm through sum-frequency generation (SFG). The up-converted beam in the UV passes through a double-grating monochromator (JY Gemini) and reaches a solar-blind photomultiplier tube (PMT). The signal intensity from the PMT is recorded by a gated photon counting technique (Becker & Hickl PMS 400A) with respect to the time delay between pump and gating pulses. The computer-controlled motorized linear translation stage (Newport IMS600) provides the minimum time delay at 8.3 fs/step. The typical response time of the system is $\Delta t = 360$ fs, shown in Fig. 1 as the t_0 pulse, which is measured by the SFG of pump scattering and gating beam; the spectral response bandwidth measured is ~ 3 nm. A fiber-coupled charge coupled device (CCD) spectrometer (Ocean Optics USB 4000) having a spectral resolution of 0.8 nm is used to simultaneously monitor the backward emission from the sample to record the steady-state spectra. The pump power (P) is controlled with a variable neutral density filter. $P = 10$ mW means that a single pulse has energy of 100 nJ or 2.0×10^{11} photons, and the corresponding pump influence and transient power density are 1.27 mJ cm⁻² and 6.37 GW cm⁻², respectively; other values of P have a linear relationship to this. An optical density (OD) = 1.0 neutral UV filter is used to attenuate the strong SF emission to avoid possible saturation of the PMT detector.

III. EXPERIMENTAL RESULTS

Figure 1 shows the behavior of the strong green emission from a 0.5-mm thick ZnTe crystal (110) at 5 K excited with a femtosecond pulse at $\lambda_{ex} = 390$ nm (3.18 eV). At very low P the bound exciton-emission lines can be recognized as two main peaks at 522 nm (2.375 eV, I1) and 525 nm (2.360 eV, I2), respectively, and a weak shoulder at 532 nm (2.331 eV, I3) [Fig. 1(a) and (b)].³² As P increases, exciting some areas of the sample, the I1 peak dominates the emission spectrum and slightly red-shifts to 522.5 nm (2.373 eV) from 521.5 nm (2.378 eV) due to a band-gap renormalization effect over the dense exciton population N [Fig. 1(a)]; the I1 line width

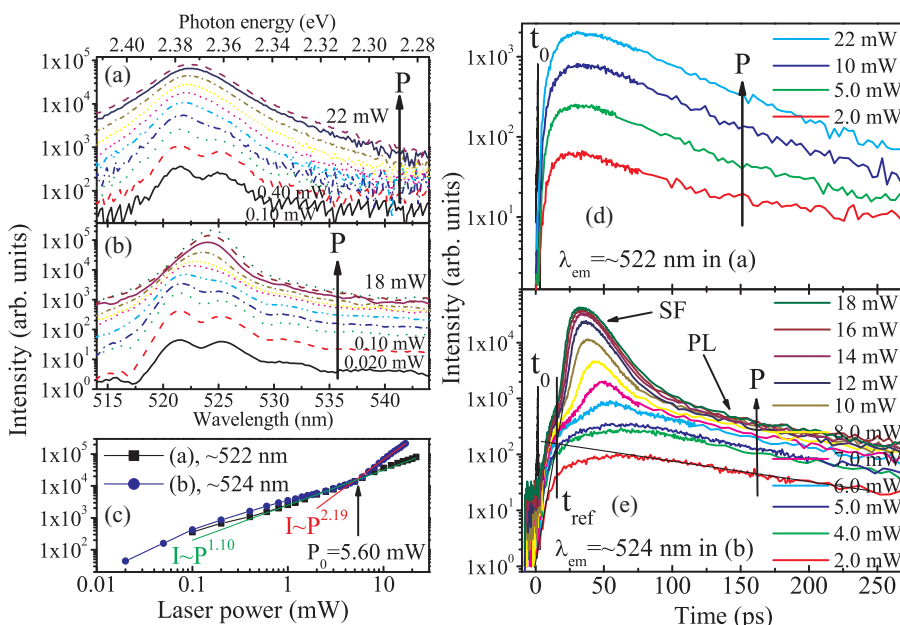


FIG. 1. (Color online) Spontaneous photoluminescence (PL) from EHP versus SF in a 0.5-mm ZnTe single crystal at 5 K excited by a femtosecond laser at $\lambda_{ex} = 390$ nm (3.18 eV). Power (P) dependent emission spectra from nonlasing and lasing areas are shown in (a) and (b), respectively. (c) P dependence of peak intensities in (a) and (b). (d) P -dependent ultrafast emission dynamics of EHP in nonlasing area, which are correspondent to (a). (e) P -dependent SF emission process in lasing area, which are correspondent to (b). t_{ref} is defined by the cross-point of build-up and decay as illustrated on 2.0 mW curve, t_0 pulse is the cross-correlation trace of excitation scattering and gating pulse, measured in far field. The arrows with P show the increase of excitation power, this applies to all subsequent figures.

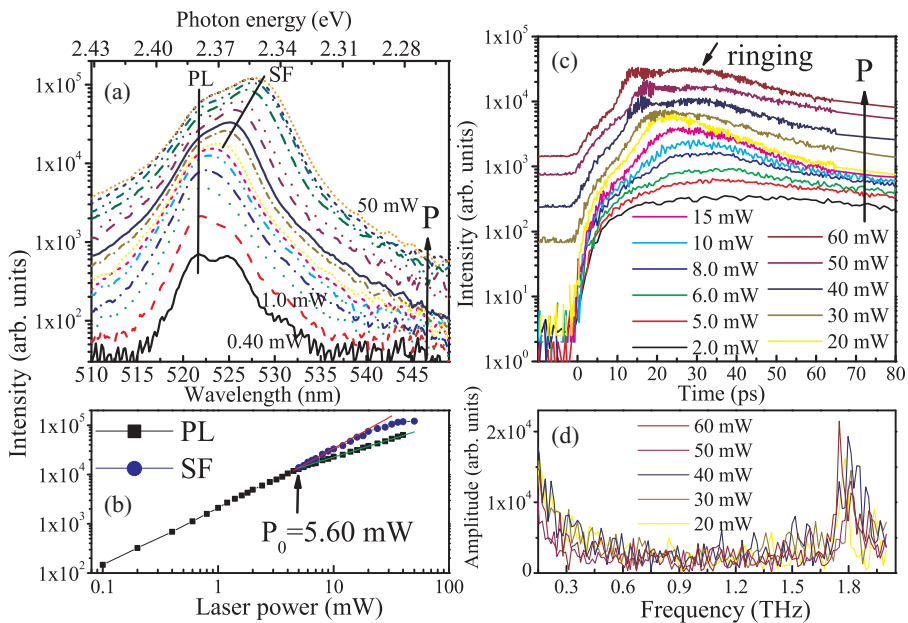


FIG. 2. (Color online) SF emission on I1 line from a 0.2-mm ZnTe single crystal at 5 K excited by a femtosecond laser at $\lambda_{\text{ex}} = 390$ nm (3.18 eV). (a) P -dependent emission spectra, the guide lines showing PL I1 peak and shift of SF peak, respectively. (b) Comparison of P dependence of peak intensities in (a). (c) P -dependent SF emission dynamics, some curves are up-shifted for clarity. (d) The corresponding FFT spectra of the curves in (c), showing the peak positions are the same for all powers.

broadens to 6.0 nm (27 meV) at 22 mW from 2.8 nm (13 meV) at low P ; the P dependence of its peak intensity, plotted in Fig. 1(c), shows a linear growth; and the corresponding ultrafast emission dynamics in Fig. 1(d) shows ordinary build-up followed by accelerated exciton recombination on P. This is typical of electron-hole plasma (EHP).¹⁶ Whereas exciting other areas of the sample, we observe the onset of lasing for the I1 line as $P > P_0$, as observed previously,³³ now the I1 peak has greatly increased intensity and undergoes a large red-shift to 524.5 nm (2.364 eV) at $P = 18$ mW, and its line width narrows to 3.2 nm (14 meV) [Fig. 1(b)]. Fitting the P dependence of peak intensities in Fig. 1(c) gives an excellent quadratic relation as $P > P_0$. The P -dependent ultrafast dynamics of lasing at ~ 524 nm (2.365 eV) are depicted in Fig. 1(e): the period from pump pulse (t_0) to build-up time (t_{ref}) represents the initial processes of carrier scattering for the release of excess energy and following exciton formation, resulting in an incoherent hot exciton population N .³⁷ At low P the curves are similar to those shown in Fig. 1(d); however, surprisingly as $P > P_0$ new high-intensity peaks emerge riding on top of the spontaneous emission with a clear time delay τ_D with respect to t_{ref} . The time delay τ_D decreases gradually from 40 ps at $P = 6.0$ mW to 10 ps at 18 mW; this is a unique characteristic of SF.^{5–11} Given a logarithmic intensity scale in Fig. 1(e) one can easily see the relatively noisy signals under moderate P compared to the curves at low P : this feature is typical of the macroscopic appearance of quantum fluctuations, again characteristic of SF, i.e., quantum noise,^{3,5} resulting from the multishot measurements.^{5,9} Furthermore at higher P (> 10 mW), regular interference fringes in the vicinity of the maximum of each curve are an observed characteristic of quantum beating of SF among multiple SF modes.^{7–9}

These observations are very reproducible; Fig. 2 shows the results from another ZnTe crystal with a thickness of 0.2 mm. As P is much higher, the SF peak sweeps through I2 and gradually red-shifts to 528 nm (2.348 eV) at $P = 50$ mW, leaving I1 behind as a shoulder [Fig. 2(a)]. The P dependence in Fig. 2(b) also indicates a clear quadratic growth in comparison to I1 as $P > P_0$. Importantly in Fig. 2(c), besides

the reduction of τ_D with P and the presence of quantum noise and fringes, each SF trace has two maxima as $P > 30$ mW: this is the characteristic ringing of SF.^{7–9} Moreover, the fringes are sufficiently clear that a beat frequency of ~ 1.8 THz can be recognized from the corresponding fast Fourier transform (FFT) spectra in Fig. 2(d), which is the difference of two SF frequencies.^{7–9} These ringing and quantum beat fringes are much clearer in a linear intensity scale, as shown in Fig. 3.

SF not only takes place on I1 but also can be observed on I2; the data recorded are shown in Fig. 4, in which the general features of SF are all observed as in Figs. 1 and 2. In this case the SF peak has a huge red-shift [Fig. 4(a)] through I3 to 540 nm (2.296 eV) at $P = 50$ mW [from 526 nm (2.357 eV) at 4.0 mW]. The P dependence of the emitted intensity shown in Fig. 4(b) also has an excellent quadratic relationship with respect to I1 as $P > P_0$. The deviation as

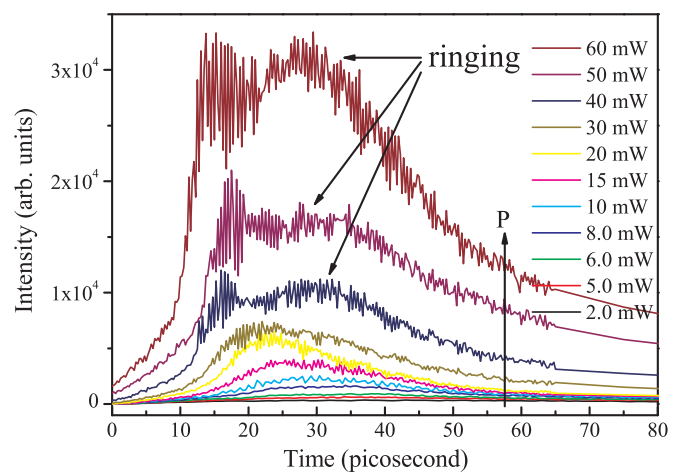


FIG. 3. (Color online) Ringing and quantum beating fringes on ultrafast SF emission dynamics on I1 line from a 0.2-mm ZnTe single crystal at 5 K. This is replotted on a linear intensity scale from Fig. 2(c) in order to show more clearly the distinct quantum beating fringes and ringing at higher P .

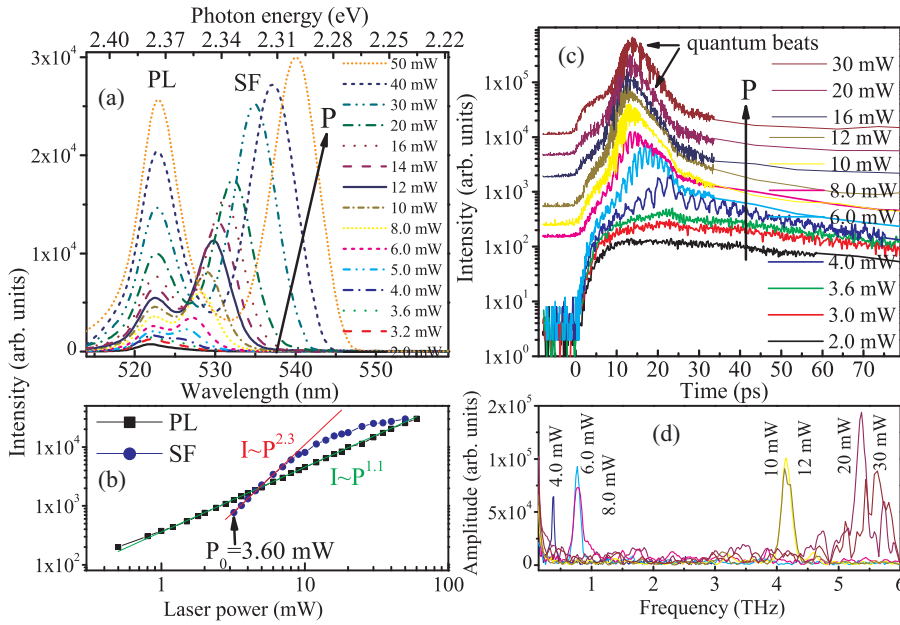


FIG. 4. (Color online) SF emission on I2 line from a 0.2-mm ZnTe single crystal at 5 K excited by a femtosecond laser at $\lambda_{ex} = 390$ nm (3.18 eV). (a) P -dependent emission spectra. (b) Comparison of P dependence of the peak intensities in (a). (c) P -dependent SF emission dynamics, some curves are up-shifted for clarity. (d) The corresponding FFT spectra of the curves in (c), showing the peak positions are dependent on P .

$P > 10$ mW is attributed to the gain saturation effect and possible damage by the high-power density of the pump laser. A most interesting feature is the P -dependent quantum beat fringes in Fig. 4(c) on a logarithmic intensity scale and Fig. 5 on a linear intensity scale and their corresponding FFT spectra

in Fig. 4(d). At moderate P the large period fringes reflect lower beat frequencies: 0.38 THz at $P = 4.0$ mW and 0.78 THz at 6.0 mW and 8.0 mW. As P increases, the fringes become dense and beating shifts to 4.15 THz at 10 mW and 12 mW; however, when $P > 12$ mW the beat frequency shifts to ~ 5.5 THz and many beats appear. This is because the multiple SF frequencies are activated as the SF peak shifts away from I2, as shown in Fig. 4(a).

SF emission weakens rapidly as temperature increases and disappears completely at ~ 45 K at the maximum P ; these are similar findings to those in Ref. 10.

IV. DISCUSSIONS

Given the previous observations, SF from the highly excited bulk ZnTe single crystals at 5 K can be confirmed unambiguously with the evidence of a clear characteristic induction time τ_D , quantum fluctuations and noise signals, quantum beating and ringing, in addition to emission line narrowing and quadratic P dependence of I_{SF} .²⁻¹¹ To the best of our knowledge such full evidence of SF in the solid state has only previously been reported in KCl:O₂^{-10,11} and not in an intrinsic semiconductor, with the key evidence in the time domain. Our observations further support those by Jho *et al.* made in the frequency domain.^{19,20}

As SF arises from N_c , a small subset of N , one can note that even at higher P the whole emission spectra does not collapse significantly into a single peak but is a mixture of SF emission from N_c and spontaneous emission from the incoherent excitons ($N - N_c$): the ultrafast emission dynamics discussed previously also show the clear difference between N_c and ($N - N_c$). These observations and the quantum beating and ringing also noted indicate that lasing here is clearly not ASE but SF; the τ_D process also excludes SR.

A. Estimation of τ_R , τ_D , N_c , and N

From the previous results we can estimate the proportion of N_c in N . The excitation laser has a spot diameter of

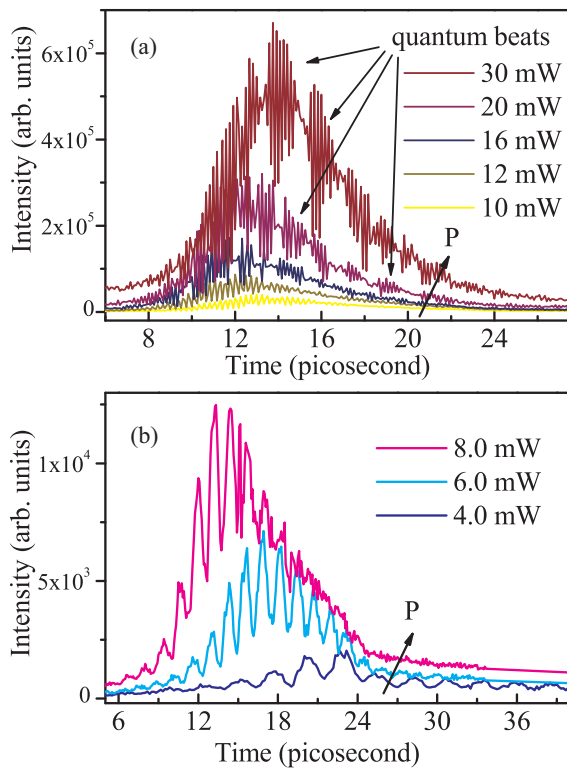


FIG. 5. (Color online) Quantum beats and beating fringes on ultrafast SF emission dynamics of the I2 line from a 0.2-mm ZnTe single crystal at 5 K. This is replotted as (a) and (b), respectively, on a linear intensity scale from Fig. 4(c) in order to show more clearly the distinct, large period quantum beat fringes at moderate P and the dense fringes and beats at higher P .

TABLE I. Some numerical results of τ_R , τ_D , and N_c .

N_c (μm^{-3})	τ_R (ps)	τ_D (ps)	$(\tau_R \tau_D)^{1/2}$ (ps)
2.0×10^4	3.66	91.9	18.3
3.0×10^4	2.44	63.7	12.5
4.0×10^4	1.83	49.2	9.49
5.0×10^4	1.46	40.2	7.67
6.0×10^4	1.22	34.1	6.45
7.0×10^4	1.05	29.6	5.57
8.0×10^4	0.915	26.3	4.90
9.0×10^4	0.814	23.6	4.38
1.0×10^5	0.732	21.4	3.96
2.0×10^5	0.366	11.4	2.04
2.1×10^5	0.349	10.9	1.95
2.2×10^5	0.333	10.5	1.87
2.3×10^5	0.318	10.1	1.79
2.4×10^5	0.305	9.67	1.72
3.0×10^5	0.244	7.89	1.39
4.0×10^5	0.183	6.07	1.05
5.0×10^5	0.146	4.95	0.851
6.0×10^5	0.122	4.19	0.715
7.0×10^5	0.105	3.64	0.617
8.0×10^5	0.0915	3.22	0.543
9.0×10^5	0.0814	2.89	0.485

$D = 100 \mu\text{m}$ and a penetration depth $l \approx 0.5 \mu\text{m}$, giving an assumed cylindrical excitation volume $V = Sl = \pi l D^2 / 4 \approx 4.0 \times 10^3 \mu\text{m}^3$. Fitting the curves at low P in Fig. 1(e) gives a typical radiative lifetime $\tau_{\text{rad}} = 120$ ps. With $\Phi \approx 10\%$, the estimated quantum yield of green emission from ZnTe at 5 K, the spontaneous emission lifetime of exciton is $\tau_{\text{SP}} \approx 1200$ ps. Using $\lambda = 524$ nm, thus $\tau_R = (8\pi/3N_c\lambda^2l)\tau_{\text{SP}} = 73\,226/N_c$ and $\tau_D = \tau_R[\ln(2\pi SlN_c)^{1/2}]^2/4 = 18\,306.6[\ln(2\pi \times 4000 \times N_c)^{1/2}]^2/N_c$, some of numerical results are listed in Table I, from which we find (i) when $\tau_D = 40$ ps at $P = 6.0$ mW, observed previously, $N_c = 5.0 \times 10^4 \mu\text{m}^{-3}$, $\tau_R = 1.5$ ps, and $(\tau_R \tau_D)^{1/2} = 7.7$ ps; (ii) for $\tau_D = 10$ ps at $P = 18$ mW, $N_c = 2.3 \times 10^5 \mu\text{m}^{-3}$, $\tau_R = 0.32$ ps, and $(\tau_R \tau_D)^{1/2} = 1.8$ ps. Given the estimated $T_2^* \approx 10$ ps for exciton in ZnTe at 5 K (see Sec. IV B), then the criterion $(\tau_R \tau_D)^{1/2} < T_2^*$ for SF is satisfied. Using $\Phi \approx 10\%$ again, and taking the photon number of a single pump pulse 2.0×10^{11} photons at $P = 10$ mW, we obtain $N \approx (10\% \times 2.0 \times 10^{11} \times 6.0/10)/V \approx 1.2 \times 10^{10}/(4.0 \times 10^3) \approx 3 \times 10^6 \mu\text{m}^{-3}$ at $P = 6.0$ mW or $N \approx 9 \times 10^6 \mu\text{m}^{-3}$ at $P = 18$ mW (similar to the order of magnitude of Mott density, $10^6 \mu\text{m}^{-3}$), yielding ratios of N_c/N as approximately 1.7% and 2.6%, respectively. More detailed analysis with a full theoretical model is underway and is not included here. Furthermore the ultrashort τ_R value in Table I indicates the line width of SF emission is a result of both the lifetime broadening and the multishot measurement; the SF pulse shape recorded thus reflects the interplay of τ_D and τ_R .

Here we clarify that the induction time is a term usually used by theorists, whereas the delay time is preferred by experimentalists, resulting from the multishot measurement and quantum fluctuation. Generally speaking both are the nearly same; hence, we use the one symbol τ_D for both

meanings for simplicity. We note some theorists use τ_D^* for delay time in experiment.³⁸

There are several criteria for SF suggested in the literature, and a dispute occurs over them among different groups.^{7-9,38} Here we adopt one of them for the purpose of clear explanation to our data; another straightforward criterion ($\tau_d < T_2^*$) is still satisfied by our data at high P but does not work at moderate P .

B. Dephasing time (T_2 or T_2^*) of exciton in ZnTe

Theoretically T_2 is the inverse of the homogeneous line width of an optical transition and is variable on temperature, whereas T_2^* is the inverse of the inhomogeneous line width and is mainly dependent on the degree of perfection of the material structure. In real materials an optical transition cannot avoid containing more or less inhomogeneous broadening due to inclusion of the defects states and impurities. The homogeneous broadening usually occupies a small portion of the total line width (Γ or $\Delta\lambda$), so the T_2 value is usually difficult to measure in experiments, for example, by zero-phonon line (ZPL) technique. Experimentally T_2^* is in general used to refer to the dephasing time by the inverse of the total line width, hence $T_2^* < T_2$. This means that T_2^* includes both homogeneous and inhomogeneous broadening, thus T_2^* can be easily estimated by $T_2^* = \lambda^2/(\Delta\lambda c) = 1240/(c\Gamma)$. Here c is the speed of light in vacuum or measured directly in time-domain by ultrafast coherent spectroscopy such as four-wave mixing (FWM) or photon-echo, coherent Raman, and free-induction decay, etc., even though the T_2 or T_2^* values obtained from different methods are usually not very consistent with each other.^{37,39} But in general T_2 times in the range 10–50 ps are obviously typical for the lowest free-exciton states in high-quality bulk (semiconductor) samples at low temperature and density.³⁹

The line width of the main emission I1 line at 521.5 nm of bound excitons in ZnTe crystals has been reported as 0.4 meV at 1.8 K and 0.7 meV at 4.2 K,^{40,41} indicating $T_2^* > 10$ ps and 5.9 ps, respectively. Given the large inhomogeneous broadening from exciton-binding effect in ZnTe and by considering an uncertainty of up to a factor of two between T_2 and T_2^* ,³⁷ then $T_2^* \approx 10$ ps at 5 K. This is very consistent with the value of 7.7 ps for $(\tau_R \tau_D)^{1/2}$ at $P = 6.0$ mW discussed previously. Also we note that a value of $T_2 \approx 25$ ps has been observed by FWM in $\text{Cd}_{0.25}\text{Zn}_{0.75}\text{Te}/\text{ZnTe}$ multiple quantum wells at 10 K.⁴² For a CdTe/ZnTe quantum dots at 7 K, $T_2 = 13$ –20 ps (by ZPL) and $T_2 = 13 \pm 3$ ps (by FWM) have been noted,⁴³ and these also suggest that the estimated $T_2^* \approx 10$ ps in ZnTe at 5 K is entirely possible.

C. SF is new evidence for spontaneous BEC of excitons

Of particular and greater significance, the occurrence of SF signifies the spontaneous macroscopic quantum coherence of an ensemble of excitons N_c formed within the clear induction time τ_D after a femtosecond excitation pulse creates thermalized incoherent excitons N . We think that the mechanism for the spontaneous coherence is the formation of a spontaneous BEC of excitons on this ultrashort timescale in the intrinsic ZnTe single crystal at 5 K.^{12-17,44,45}

BEC is the macroscopic population of one quantum mechanical state by non- or weakly interacting Bose particles in thermal (quasi-)equilibrium. A single exciton consists of two spin $1/2$ particles (one electron and one hole), so its total spin is either 0 (singlet) or 1 (triplet). This means that a singlet exciton is a boson (or called a boson-like quasiparticle by some authors), therefore singlet excitons can form a spontaneous BEC of weakly interacting bosons. A BEC of excitons occurs only if both the temperature is below a critical temperature (T_c) and the exciton density N is raised above a critical density (n_c), which is close to, or above, the Mott density (N_{Mott}). The mass of an exciton is comparable to a free electron; this makes T_c higher (even up to room temperature), and the N can be created easily at densities exceeding $10^6 \mu\text{m}^{-3}$ (similar order to N_{Mott}) by pulsed laser excitation.

As mentioned in the Introduction, one of the key issues for the observation of a BEC of excitons focuses on the spontaneous macroscopic quantum coherence of excitons;¹⁷ SF from coherent excitons in a semiconductor provides an excellent opportunity for this. In SF the quantum ensemble of coherent excitons N_c (on a single quantum state) forms with a characteristic induction time (τ_D) on an ultrafast timescale from the incoherent hot excitons N in a dense system in population inversion; this satisfies the partial coherence of bosons (excitons) with N_c/N , predicted by Bose-Einstein statistics,¹⁸ and directly means that N must be close to, or above, N_{Mott} . Inevitably, this ensemble of coherent excitons N_c is not in a stable state and can very easily be stimulated (triggered) by a random spontaneous emission inside the excitation volume V , tipping mechanism of SF.³ This then gives rise to SF-emission pulses at a recombination rate quadratically increasing as N or P ³; this usually is observed as mirrorless lasing in experiments. Here, one should notice again that SF clearly differs from the other lasing mechanisms of either SR or ASE, because both SR and ASE lack a τ_D , which is characteristic of SF.²⁻⁴

The ultrafast τ_D process and quantum beating need higher time-resolution measurements and are difficult to resolve by an ordinary ultrafast spectroscopic technique such as the streak camera^{23,28,30,33} or the optical Kerr-gate method.^{24,25,27} In the latter case the weak signal intensity greatly reduces the contrast ratio between spontaneous emission and SF; furthermore, its existing residual system time delay makes it hard to distinguish τ_D from other processes, hence most of SF claims previously made were not substantiated by the experimental evidence provided. On the other hand the spontaneous lifetime of an exciton (τ_{SP}) is relatively short (~ 1 ns for singlet exciton), the complicated exciton scattering processes always decrease the quantum yield (Φ) of exciton luminescence and make the observed radiative lifetime (τ_{rad}) of excitons emission much shorter,³⁷ whereas the release time of SF pulse (τ_R) is ultrashort compared to τ_{SP} and τ_{rad} , usually shorter than a few picoseconds (see Table I). This ultrashort τ_R implies that the line width of SF emission must be lifetime broadened due to the quantum uncertainty principle. By ignoring this lifetime broadening effect, some of the previous observations of BEC of excitons have been focused on the very sharp emission lines.^{13,14}

The third point that deserves mention is that the decoherence (dephasing) process opposes the spontaneous coherence:

it always acts to destroy the coherence so τ_D in SF is always limited by T_2^* and the observation of BEC of excitons must consider T_2^* values of the materials used. In view of the previous discussions, the BEC of excitons is inevitably deemed to emit SF from the excitonic condensate and is observable in experiments by the ultrahigh time-resolution technique.

Under our experimental conditions within the small excitation volume ($V \approx 4.0 \times 10^3 \mu\text{m}^3$) in some regions of the crystal bulk, a high density ensemble of bound excitons can form having sufficiently long T_2^* that spontaneous symmetry breaking within a time τ_D forms a spontaneous coherence in a single quantum state I1 or I2, i.e., a spontaneous BEC of excitons forms. The whole coherent system then, being triggered by a random spontaneous emission event, yields a burst of observable SF pulses when the coherent exciton density N_c exceeds a critical density n_c as $P > P_0$. This case is clearly different from the so-called driven-BEC of exciton-polaritons in the microcavities,¹⁵⁻¹⁷ where the excitons and photons are confined together by the cavity effect to mix with each other to form forced coherence.

D. Temperature effect of SF from BEC of bound excitons

We have tried to measure the temperature dependence of the SF from BEC of bound excitons in ZnTe crystal. As temperature increases both the PL and SF emission of ZnTe quickly undergoes a red-shift,⁴⁶ which is a result of a band gap expansion effect, and the corresponding up-conversion signal is beyond the detection range of our UV PMT, thus we can only monitor the emission with a CCD spectrometer and notice that SF emission disappears completely above ~ 45 K at $P = 50$ mW. This could possibly be due to a damage effect in the material by the high laser power given that the power density of $> 30 \text{ GW cm}^{-2}$ at $P = 50$ mW causes damage to most materials in the strong linear absorption band. Another possible cause is that the band expansion effect leads to the bound exciton states gradually shifting toward the deep conduction band, hence they drown in the EHP, where a high N_c is difficult to reach due to the increasing exciton-exciton annihilation rate and the greatly reduced T_2^* . Even so, we are still able to clearly observe SF emission from ZnTe up to ~ 45 K; this implies that the bound excitons still can form spontaneous coherence at the bottom of conduction band where the EHP density is not very high. Furthermore, because the inhomogeneous broadening in an optical transition is not as sensitive to temperature as the homogeneous broadening, the real $N_c/N \sim$ temperature relation does not strictly follow the relation for an ideal case.

E. Binding impurities and defect states in ZnTe

The bound-exciton emission from ZnTe materials has been studied and confirmed in many earlier reports: The I1 line is from the exciton bound to a neutral acceptor (zinc vacancy), whereas the I2 line is the exciton bound to a neutral donor.^{32,40,46,47} Due to the many sharp spectral lines contained

in the vicinity of the band-edge of ZnTe at ~ 5 K, which cannot be clearly resolved by our CCD spectrometer, the weak-shoulder I3 line tentatively cannot be clearly identified according to the earlier papers.^{40,46} The exciton-emission spectrum from these commercial ZnTe single crystals is always accompanied by a red band at ~ 625 nm–725 nm (1.98 eV–1.71 eV) (not shown here), indicating the existence of impurities and defect states, which has been extensively observed and studied previously.^{41,48} One of the authors has also observed similar effects by the impurities and defect states in a ZnO single crystal,^{49,50} that is, an analogy of the ZnTe structure. With only our optical spectroscopic data, we presently cannot clearly point out the kind of optically active impurities and defect states involved in the transitions observed; these are primarily dependent on the growing method and conditions. We also noticed that one paper has systematically studied the emission from ZnTe upon growing conditions,⁴¹ indicating the clear impurities effects to the emission from both bound excitons and impurities and defect states.

In our observations the saturation effect of these impurity and defect states to high P is obvious in Fig. 2(b) and Fig. 4(b) by the clear deviation as $P > 10$ mW. We see especially in Fig. 4(b) the SF emission > 535 nm is observed from the band tail where the impurities and defect states dominate. Here SF emission and the density of impurities and defect states are connected together by the inherent dephasing time (T_2^*), the exceedingly high-density impurities and defect states in bad quality ZnTe crystals will greatly reduce the T_2^* , hence killing SF emission. On the other hand the power-dependent PL emission does not have a clear deviation as $P > 10$ mW in these curves, as the PL is determined by the total density of excited states and is not sensitive to T_2^* .

From our data the saturation threshold is approximately at $P = 10$ mW; by the photon density of the pump laser $N_p = 5.0 \times 10^6 \mu\text{m}^{-3}$ at $P = 10$ mW and the quantum yield $\Phi \approx 10\%$, we estimate the density of impurity and defect states is approximately $N_{\text{im}} \approx 5.0 \times 10^5 \mu\text{m}^{-3}$, which is apparently larger than $N_c = 2.3 \times 10^5 \mu\text{m}^{-3}$ at $P = 18$ mW obtained previously in Sec. IV A. This indicates that the density of impurities and defect states N_{im} , to which the excitons are bound in the excitation volume V , plays a role of providing a population density to the ensemble of coherent excitons N_c in SF. Whereas the incoherent excitons ($N - N_c$) responsible for PL emission are bound to other random impurities and defect states ($N_{\text{im}} - N_c$), which cannot provide sufficiently large population density for SF. Further, given that many sharp spectral lines are contained in the vicinity of the band-edge of ZnTe indicating that rich impurities and defect states exist in this spectral region,⁴⁷ it is reasonable that the excitons N_c can be simultaneously bound to two or more specific states provided they have appropriate population density and T_2^* to support SF; as a direct consequence, two such discrete-binding states can yield independent SF resulting in the interference fringes of quantum beating on the time domain curves, as in Fig. 3 and Fig. 5. Thus in Fig. 4(d) the appearance of multiple beating frequencies are attributed to the different binding states activated as SF emission undergoes large red-shift in Fig. 4(a), and the variation of beating frequencies directly reflects the change of energy difference between two activated SF states.

F. Possibility of BEC of free excitons and superfluidity

Following the discussions on binding effect in Sec. IV E, we conclude that the easy inclusion of impurities and defect states in the wide-band semiconductor materials³⁹ and that in a material the free exciton always has slightly higher energy than the bound exciton by a binding energy, which is usually ~ 1 meV to ~ 200 meV for shallow donors and acceptors.³⁹ As a result of this, the bound excitons are preferentially populated during exciton thermalization and usually dominate the whole emission at low temperature,³⁷ whereas the free excitons only contribute a tiny portion of emission,^{41,46,47} therefore a spontaneous BEC of bound excitons is relatively easy to form, as in our previous observations, and it is a big challenge to observe SF emission from a spontaneous BEC of free excitons at low temperature. However, it is fully conceivable to achieve this in very high-quality materials in which the free excitons dominate the whole emission, and the density of bound excitons should be lower than $10^4 \mu\text{m}^{-3}$. This density is not sufficiently high enough to support SF from our experimental estimations in Secs. IV A and IV E, although the T_2^* does not change with a low density of impurities and defect states. In this case for free excitons with the inhomogeneous broadening greatly reduced, the homogenous broadening therefore dominates, the formation of a spontaneous coherence is then mainly controlled by T_2 and not T_2^* , and a nearly ideal $N_c/N \sim$ temperature relation could be observed. By definition a bound exciton straightforwardly means a localized exciton that cannot migrate freely in a crystalline structure, whereas a free exciton can,^{37,39} thus the characteristic superfluidity is not expected from a spontaneous BEC of bound excitons, yet promisingly could occur in a spontaneous BEC of free excitons.

V. CONCLUSIONS

We have observed clear evidence of SF in bulk ZnTe crystals between 5 K and 45 K under femtosecond laser excitation. A clear characteristic induction time, τ_D , together with quantum noise and quantum beating and ringing support this unambiguous observation of SF emission. We put forward that this is also new evidence that a spontaneous BEC of excitons has formed, which then spontaneously decays to yield the SF burst, and so it is the process of spontaneous Bose condensation that governs the formation of the coherent ensemble of excitons in the ZnTe crystals on an ultrafast timescale. Our case is clearly different from other cases of driven-BEC. The decoherence factor T_2^* , which is related to the degree of perfection of the crystal structure, must be considered in achieving BEC of excitons. The careful use of femtosecond time-resolution techniques to identify the SF process on an ultrafast timescale should enable future experimental studies in other semiconductor materials.

ACKNOWLEDGMENT

We thank R. A. Abram and J. M. Chamberlain for fruitful discussions and critical review.

*Corresponding author: dechang.dai@dur.ac.uk

- ¹R. H. Dicke, *Phys. Rev.* **93**, 99 (1954).
- ²R. Bonifacio and L. A. Lugiato, *Phys. Rev. A* **11**, 1507 (1975).
- ³Q. H. F. Vreken, M. F. H. Schuurmans, and D. Polder, *Nature* **285**, 70 (1980).
- ⁴A. E. Siegman, *Lasers*, (Univ. Science Books, California, 1986), Chap. 13.8, p. 547.
- ⁵J. Okada, K. Ikeda, and M. Matasuoka, *Opt. Commun.* **27**, 321 (1978).
- ⁶N. Skribanowitz, I. P. Herman, J. C. MacGillivray, and M. S. Feld, *Phys. Rev. Lett.* **30**, 309 (1973).
- ⁷M. S. Feld and J. C. MacGillivray, *Top. Curr. Phys.* **21**, 7 (1980).
- ⁸M. F. H. Schuurmans, Q. H. F. Vreken, and D. Polder, *Adv. Atom. Mol. Phys.* **17**, 167 (1981).
- ⁹Q. H. F. Vreken and H. M. Gibbs, *Top. Curr. Phys.* **27**, 111 (1982).
- ¹⁰M. S. Malcuit, J. J. Maki, D. J. Simkin, and R. W. Boyd, *Phys. Rev. Lett.* **59**, 1189 (1987).
- ¹¹R. Florian, L. O. Schwan, and D. Schmid, *Phys. Rev. A* **29**, 2709 (1984).
- ¹²J. M. Blatt, K. W. Boer, and W. Brandt, *Phys. Rev.* **126**, 1691 (1962).
- ¹³A. Griffin, D. W. Snoke, and S. Stringari, eds., *Bose-Einstein Condensation* (Cambridge Univ. Press, Cambridge, UK, 1995).
- ¹⁴S. A. Moskalenko and D. W. Snoke, *Bose-Einstein Condensation of Excitons and Biexcitons and Coherent Nonlinear Optics with Excitons* (Cambridge Univ. Press, Cambridge, UK, 2000).
- ¹⁵D. Snoke, *Science*, **298**, 1368 (2002).
- ¹⁶C. Klingshirn, in *Frontiers of Optical Spectroscopy*, edited by B. Di Bartolo and O. Forte (Kluwer Acad. Pub., Netherlands, 2005), Chap. 15, p. 539.
- ¹⁷D. Snoke, *Nature*, **443**, 403 (2006).
- ¹⁸J. F. Annett, *Superconductivity, Superfluids and Condensates* (Oxford Univ. Press, Oxford, UK, 2004).
- ¹⁹Y. D. Jho, X. Wang, J. Kono, D. H. Reitze, X. Wei, A. A. Belyanin, V. V. Kocharovskiy, V. V. Kocharovskiy, and G. S. Solomon, *Phys. Rev. Lett.* **96**, 237401 (2006).
- ²⁰Y. D. Jho, X. Wang, D. H. Reitze, J. Kono, A. A. Belyanin, V. V. Kocharovskiy, V. V. Kocharovskiy, and G. S. Solomon, *Phys. Rev. B* **81**, 155314 (2010).
- ²¹M. H. F. Overwijk, J. I. Dijkhuis, and H. W. de Wijn, *Phys. Rev. Lett.* **65**, 2015 (1990).
- ²²P. P. Vasil'ev, *Rep. Prog. Phys.* **72**, 076501 (2009).
- ²³C. R. Ding, W. Lin, B. C. Chen, F. L. Zhao, J. W. Dong, M. Shi, H. Z. Wang, Y. F. Hsu, and A. B. Djuricic, *Appl. Phys. Lett.* **93**, 151902 (2008).
- ²⁴S. Mitsubori, I. Katayama, S. H. Lee, T. Yao, and J. Takeda, *J. Phys.: Condens. Matter* **21**, 064211 (2009).
- ²⁵J. Takeda, N. Arai, Y. Toshiue, H. J. Ko, and T. Yao, *Jpn J. Appl. Phys.* **45**, 6961 (2006).
- ²⁶W. L. Zhang, L. Chai, Q. R. Xing, Q. Y. Wang, K. S. Wong, P. Yu, H. Wang, Z. K. Tang, and G. W. L. Wong, *Chinese Phys. Lett.* **16**, 728 (1999).
- ²⁷K. Miyajima, Y. Kagotani, S. Saito, M. Ashida, and T. Itoh, *J. Phys.: Condens. Matter* **21**, 195802 (2009).
- ²⁸J. Y. Luo, N. S. Xu, F. L. Zhao, S. Z. Deng, and Y. T. Tao, *J. Appl. Phys.* **109**, 024312 (2011).
- ²⁹P. V. Zinov'ev, S. V. Lopina, Yu. V. Naboikin, M. B. Silaeva, V. V. Samartsev, and Yu. E. Sheibut, *Sov. Phys. JETP* **58**, 1129 (1983).
- ³⁰H. Z. Wang, X. G. Zheng, F. L. Zhao, Z. L. Gao, and Z. X. Yu, *Phys. Rev. Lett.* **74**, 4079 (1995).
- ³¹F. Sasaki, S. Kobayashi, S. Haraichi, H. Yanagi, S. Hotta, M. Ichikawa, and Y. Taniguchi, *Jpn J. Appl. Phys.* **45**, L1206 (2006).
- ³²M. S. Brodin and M. G. Matsko, *Solid State Commun.* **25**, 789 (1978).
- ³³F. A. Majumder, H. Kalt, C. Klingshirn, H. Stanzl, and W. Gebhardt, *Phys. Stat. Sol. B* **188**, 191 (1995).
- ³⁴H. Mahr and M. D. Hirsch, *Opt. Commun.* **13**, 96 (1975).
- ³⁵J.-C. Diels and W. Rudolph, *Ultrashort Laser Pulse Phenomena: Fundamentals, Techniques, and Applications on a Femtosecond Time Scale* (Academic, London, 1995), p. 419.
- ³⁶C. Rulliere, T. Amand, and X. Marie, in *Femtosecond Laser Pulses: Principle and Experiments*, edited by C. Rulliere (Springer, New York, 2005), Chap. 8, p. 252.
- ³⁷J. Shah, *Ultrafast Spectroscopy of Semiconductors and Semiconductor Nanostructures* (Springer, Berlin, 1999), Chaps. 1, 2, 6, and 9, pp. 1, 27, 225, and 325.
- ³⁸V. V. Zheleznyakov, V. V. Kocharovskii, and V. V. Kocharovskii, *Sov. Phys. Usp* **32**, 835 (1989).
- ³⁹C. F. Klingshirn, *Semiconductor Optics* (Springer, Berlin, 1997), Chap. 22, p. 339.
- ⁴⁰A. Opanowicz, K. Marinova, H. Liebing, and W. Ruppel, *Phys. Stat. Sol. B* **75**, 471 (1976).
- ⁴¹M. Nishio, H. Ogawa, T. Nishinaga, and M. Washiyama, *Jpn. J. Appl. Phys.* **25**, 1470 (1986).
- ⁴²R. P. Stanley, J. Hegarty, R. Fischer, J. Feldmann, E. O. Gobel, R. D. Feldman, and R. F. Austin, *Phys. Rev. Lett.* **67**, 128 (1991).
- ⁴³B. Patton, W. Langbein, U. Woggon, L. Maingault, and H. Mariette, *Phys. Rev. B* **73**, 235354 (2006).
- ⁴⁴D. W. Snoke, *Phys. Stat. Sol. B* **238**, 389 (2003).
- ⁴⁵D. Snoke, *Nature Phys.* **4**, 674 (2008).
- ⁴⁶C. F. Klingshirn, W. Maier, B. Honerlage, H. Haug, and S. W. Koch, *Solid State Electron.* **21**, 1357 (1978).
- ⁴⁷W. Wardzynski and K. Pataj, *Phys. Stat. Sol. B*, **75**, 341 (1976).
- ⁴⁸See, e.g., R. E. Dietz, D. G. Thomas, and J. J. Hopfield, *Phys. Rev. Lett.* **8**, 391 (1962).
- ⁴⁹D. C. Dai, S. J. Xu, S. L. Shi, M. H. Xie, and C. M. Che, *Opt. Lett.* **30**, 3377 (2005).
- ⁵⁰D. C. Dai, S. J. Xu, S. L. Shi, M. H. Xie, and C. M. Che, *IEEE Photon. Tech. Lett.* **18**, 1533 (2006).